

Laser effects on porous silicon synthesis by photoelectrochemical etching process

A. RAMZY*, K. OMAR, Z. HASSAN, H. ABU HASSAN

School of Physics, Universiti Sains Malaysia, 11800 USM, Penang, Malaysia

Porous silicon (Si) structure has been produced by photoelectrochemical etching process, which shows strong room temperature luminescence in the red region. The properties of the nanostructures from three etched samples are presented. The etching mechanism has been investigated and it is found to produce different nanostructures for different illumination sittings. It has been observed that the etching process starts under S-band photon. The formation of defects in porous Si etched samples before and after laser irradiation has been studied by scanning electron microscope (SEM). The morphology studies showed the effect of laser power on the porous Si which indicated that the structure has been destroyed and no more optical and electrical properties could be achieved from these due to this effect. This mechanism has been confirmed by X-ray diffraction (XRD) results.

(Received September 20, 2009; accepted October 29, 2009)

Keywords: Laser effect, Porous silicon, Nd:YAG laser

1. Introduction

Porous silicon has been suggested as possible candidate for silicon-based optoelectronics due to its remarkable luminescence properties. The Canham discovery of intense visible light emission from porous silicon has stimulated a wealth of investigations in order to understand the physical mechanisms responsible for this novel feature [1-2]. The microstructural, chemical, electronic, and optical properties of porous silicon have been extensively studied by various experimental techniques. Since 1990s, some morphological and structural studies have been devoted to the understanding of the origin of this photoluminescence emission at energies far above the band gap of bulk silicon (1.1eV) and with intensity unexpected for indirect band gap materials. However, quantum confinement model is the one of the more realistic model to explain the origin of photoluminescence [3-4]. According to this model, carriers are confined in silicon nanocrystallites produced by the electrochemical etching. Thus, an increase of the band gap is induced. When using a UV or blue light excitation, it is possible to emit visible light from porous layer. The quantum confinement model in nanocrystallites size leads to the shift of the band gap from the near-infrared wavelength region to the visible range. In this model, the position of the luminescence peak and its efficiency are only dependent on the size and shape of silicon nanocrystallites [4-5].

There are several etching techniques that can be used to produce porous silicon. This work used electrochemical anodization method under the illumination of light to fabricate luminescent porous silicon [6-7]. The study of laser effects on porous Si is important for the investigation of surface defects, and optical and electrical properties, based on the principle of the laser-semiconductor interaction which is a very interesting process in industrial

applications (welding, drilling, etc...).

2. Experimental setup

A photoelectrochemical cell has been used to fabricate the porous silicon. The cell has two-electrode system with a silicon wafer anode and platinum cathode. The electrolyte used is HF: ethanol in the ratio of 1: 4. The electrolyte provided the medium for the moving electrons. The position of the lamp has to be adjusted so that the silicon wafer can gain as much photon as possible. Anodization was carried out at current densities values of 30, 60 and 100 mA/cm² and for duration of about 30 minutes. After anodization the porous silicon samples were dried under nitrogen shower.

The global anodic semi-reaction during pore formation can be written as [8]



In this work, porous silicon samples were prepared by anodic etching of n-type c-silicon under illumination of light for different current densities 30, 60 and 100 mA/cm². The surface morphology and the optical properties of porous Si were studied using SEM, Raman spectroscopy and photoluminescence (PL). Subsequently, the samples were exposed to Nd:YAG laser (1.06 μm) at pulse duration of 300 μs to create the defects, and their morphological properties investigated using the SEM, and sheet resistance measured for electrical properties.

3. Results and discussion

It is observed that after etching, the surface of the wafer became rough due to the creation of a network of

pores inside the materials. Raman scattering spectroscopy is one of the powerful techniques for studying structure related information. The Raman spectrum is the plot of the intensity of scattered light versus the energy difference. The line shape analysis of the first order Raman mode provides the information of the characteristic dimensions. This also means that the Raman peak shape is highly dependent on the nanostructure shape and size parameters of nanocrystals. Photoluminescence is one of the properties of nanostructured materials. In order to explain the broad photoluminescence band, it is assumed that the porous silicon contains wide distribution of nanocrystallites with different sizes. This means that the

position and shape of the photoluminescence band also depends on the size distribution of the nanocrystallites.

3.1 Surface morphology

The pore diameter has been deduced to be approximately 0.50 - 0.62 μm for current density of 30 mA/cm^2 . The average pore size is 0.54 μm . The pores size of the sample is not uniform. Fig. 2 shows spherical shapes dimension. However, some of the pores also appeared as square-like and elongated shapes. Moreover, the surface of the porous silicon consisted of discrete pores with smooth walls, and with short branches pores.

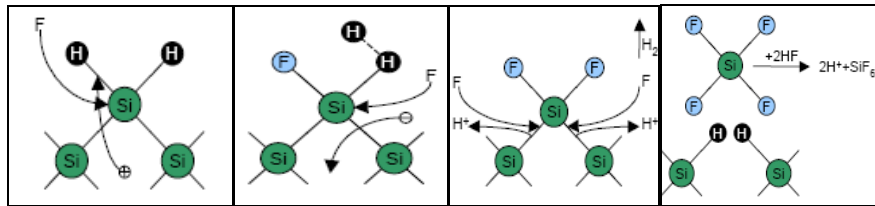


Fig. 1. The anodic semi-reaction of silicon.

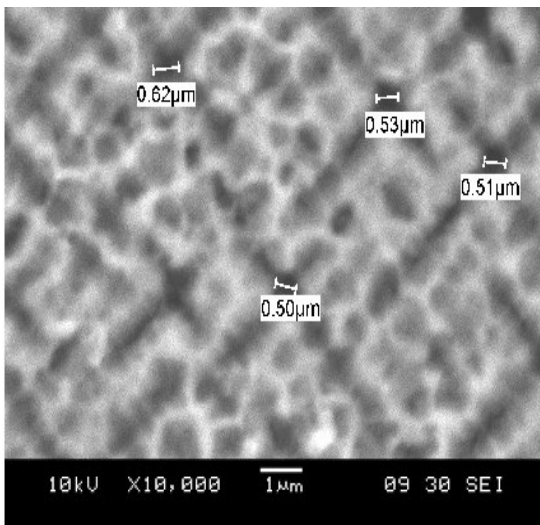


Fig. 2. Plan view SEM micrograph of porous silicon prepared with current density of 30 mA/cm^2 .

The etched sample with higher current density of 60 mA/cm^2 has different porous morphology as shown in Fig. 3. The pores size of the sample is random and it is found to be in the range of 0.69 - 0.91 μm . The plan view SEM image of porous silicon prepared with current density of 100 mA/cm^2 is shown in Fig. 4. It is observed that the surface morphology of this sample is dissimilar to previous samples. The pores size is approximately 0.54 - 1.68 μm . The pores size appeared to be larger. On the other hand, the pores are distributed densely and randomly. The pores have spherical shapes dimension. However, some pores shapes are square-like and elongated.

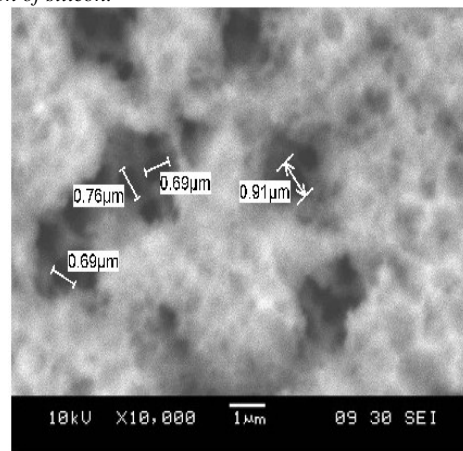


Fig. 3. Plan view SEM micrograph of porous silicon prepared with current density of 60 mA/cm^2 .

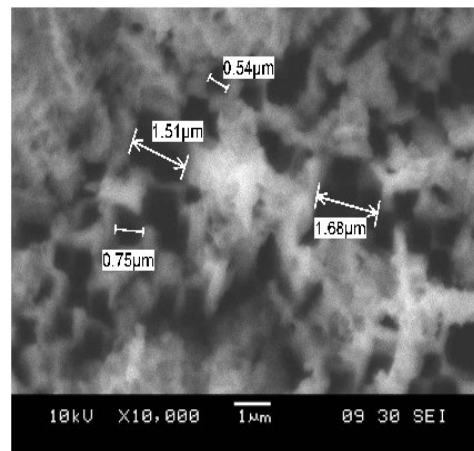


Fig. 4. Plan view SEM micrograph of porous silicon prepared with current density of 100 mA/cm^2 .

Higher current densities showed bigger pores diameters than that at lower current densities. Therefore, the pore diameter is increased by increasing the current density. The three samples are categorized as macropores with average pore diameters of > 50 nm according to International Union of Pure and Applied Chemistry (IUPAC) [4]. The pores are distributed randomly at different locations. The pores size of the sample is not uniform. Therefore it is believed that pore diameter and micro structure are dependent on anodization conditions such as HF concentration, duration time, temperature, and current density [9]. Moreover, it does not always produce similar surface morphology by this electrochemical etching technique.

3.2 Raman spectroscopy

The Raman spectrum of crystalline silicon (c-Si) is shown in Fig. 5. It is highly symmetric, and has a full width at half maxima (FWHM) of 2.7 cm^{-1} . As the grain size in microcrystalline silicon decreases, the Raman shift decreases, the FWHM increases, and the peak becomes increasingly asymmetric with an extended tail at low frequencies. It is observed to be very broad, which indicates the absence of the amorphous phase in porous silicon samples. The peak shift is increasing showing that the Raman shift is red shifting and this shifting corresponds to a relaxation of compressive stress. This type of relaxation is known as compressive stress relaxation due to the presence of pores.

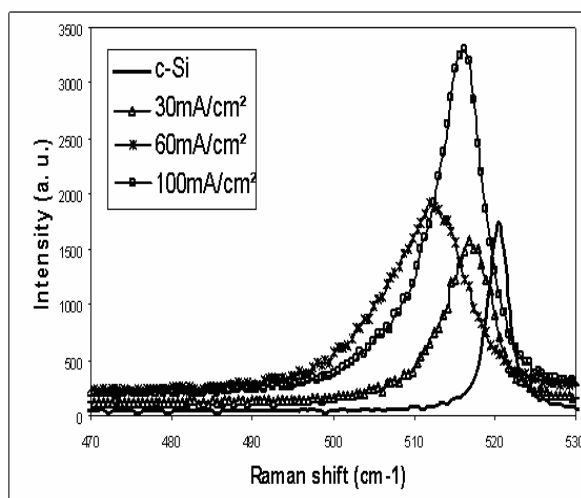


Fig. 5. Raman spectra of light-emitting porous silicon samples for current density of 30, 60 and 100 mA/cm².

The silicon nanocrystallites relax the wavevector selection rule and cause the Raman spectrum to broaden, red shift, and become asymmetric. Crystal translational symmetry leads to plane wave phonon eigenstates. The phonon, which is involved in first-order Raman scattering, have $q=0$ at the Brillouin zone center (Γ point). When the size of the particles reduces to the order of nanometer, the wave function of optical phonons will no longer be a plane

wave. A relaxation rule of the wave vector conservation is due to the localization of wave function. Those with $q>0$ can take part in the Raman scattering process, leading to a red shift and broadening of the Raman peak [10].

3.3 Photoluminescence

The photoluminescence spectroscopy for different current densities of porous silicon is shown in Fig. 6. The peak position is blue shift from 688.7 nm to 655.5 nm as current density increases from 30 A/cm² to 100 A/cm². The result of shifting toward shorter wavelength is due to the diminishing quantum confinement dimension of the skeleton in the sample [11]. It meant blue shift of wavelength as anodizing current increases and porosity increases as well. The photoluminescence is assigned to S band if its peak wavelength is in the range of 400 – 800 nm. The result shows that the peak wavelength is in the range of 655.5 – 688.7 nm, indicating that this photoluminescence is S-band luminescence. According to the quantum confinement luminescence model, the shorter peak wavelength of luminescence is due to increasing energy band gap of the porous structure [12]. The result shows that the energy band gap is increased from 1.806 eV to 1.892 eV as the current density increases from 30 to 100 mA/cm². The energy band gap of crystalline silicon is 1.12 eV and the energy band gap of porous silicon is increased up to 1.8 eV. The particles are confined into lower dimension when the materials get to lower dimensions confinement. The probability of the recombination of the electrons and holes is higher in low-dimensional structure. This leads to a higher efficiency and higher energy.

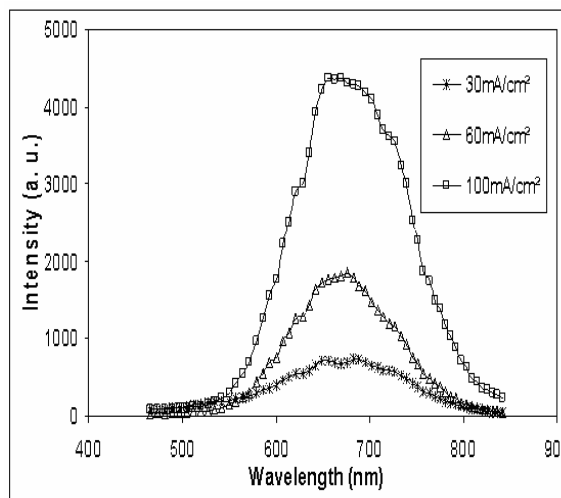


Fig. 6. The photoluminescence spectra for different current densities of porous silicon.

The room temperature photoluminescence intensity shows an increasing trend with current density. The strengths of photoluminescence output become stronger as the porosity increased. This means that, the intensity of photoluminescence is proportional to the number of photons emitted by the porous surface. There is a dramatic

rise in photoluminescence intensity as the porosity rise from 0 – 77% with increase the current density from 30 mA/cm² to 100 mA/cm². The photoluminescence intensity is directly affected by the current density and so as current density is large more luminescent porous silicon is obtained. The higher energy is dominated by surface-state recombination and low energy emission originates from the quantum confinement effect [13].

4. The effect of laser on porous silicon structure

The measurement showed the electrical resistance of surface at laser energy density of 0.75 J/cm² is $1 \times 10^3 \Omega/\text{cm}^2$ and at laser energy density of 1.25 J/cm² it is $13 \times 10^3 \Omega/\text{cm}^2$. The depths of penetration are also increased and proportional to the irradiation energy density, and were 120 μm and 470 μm at the same laser energy densities, respectively. An increase in laser energy density leads to an increase in the penetration depth which could be due to increase in the structural defects as a result of rapid re-sclerosing which tend to locate these defects at the surface. These defects act as recombination centers or trapping centers, which are represented by deep energy levels within silicon energy gap, which will reduce the electrical connectivity and thereby increase the surface resistance [14-15].

The peak of laser energy density (E.D.) of 0.75 J/cm² is represented as a deterioration in the crystalline characteristics of the region irradiated, as shown in Fig. 7 (a) where there has been a substantial decrease in the severity of the summit at ($2\theta = 90^\circ$), which gave an indication of a phase shift of the region of the irradiated area from porous shape to amorphous. This is due to the high energy irradiation which caused melting and then quick re-hardening and has not been able to re-crystallize in the short time. The increase of the laser power density to 1.25 J/cm² has shown that the structure turned to amorphous as shown in Fig. 7 (b).

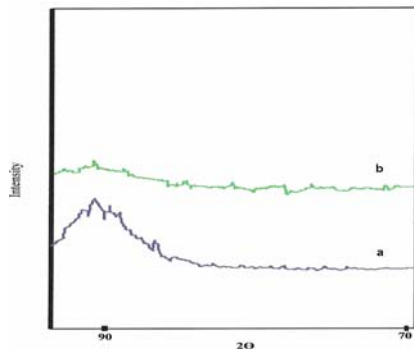


Fig. 7. XRD of porous Si, (a) with 0.75 J/cm² of laser power density (b) with 1.25 J/cm².

The induced damage has had varying shapes and depths according to the irradiation conditions. The linear cracks and fractions appeared at irradiated area as a result of laser energy density of 0.25 J/cm², and then these cracks disappeared at the center of irradiated area because the threshold laser energy depends on the pulse duration,

which meant that the existed cracks were due to thermal shocks. The absorption energy leads to the temperature gradient which shows that the hardness of the crystal surface is less than the crystal itself. On the other hand, it could be explained that these defects are dependent on thermal shocks due to the rapid heating and cooling, which caused these pressure stresses. The reason for this disappearance at the center of irradiated area is related to the temperature gradient as shown in Fig. 8.

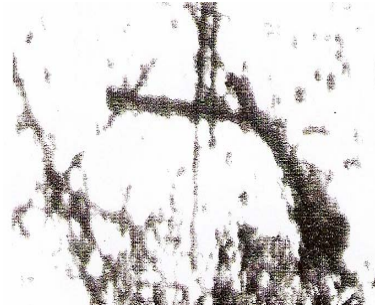


Fig. 8. PS irradiated using E.D. 0.25 J/cm².

The irregular spherical shape is formed due to the Gaussian pattern of the laser beam incident at 0.75 J/cm². It started to melt the surface, as shown in Fig. 9, and at laser energy density of 1.25 J/cm² it started to form large crack and concave area surrounded by circular lines. This could be explained by the fact that the laser irradiation is the process of accumulation of heat leading to rising in temperature from melting temperature to evaporation temperature, which leads to the generation of steam spray which caused the edge of the concavity of the molten crystal [16-17]. The emergence of this damage included nipples and some spherical drops as shown in Fig. 10 [18].

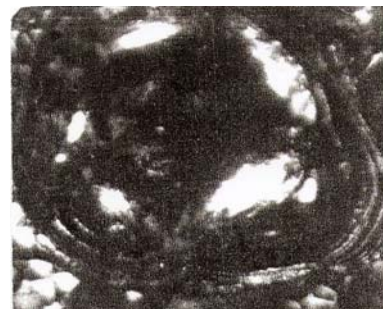


Fig. 9. PS irradiated using E.D. 0.75 J/cm².

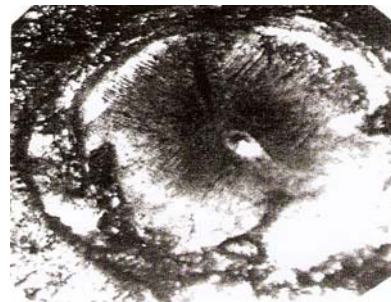


Fig. 10. PS irradiated using E.D. 1.25 J/cm².

The reluctance of evaporation was mainly adopted due to an apostate pressure of vaporized material and this pressure generated by the first part of the laser pulse while the later part of the laser pulse caused super heating that could be generated by a secondary evaporation front phase with a high pressure applied on the surface. It can be said that the spherical drops is resulted due to the initial evaporation process and the nipples due to the secondary evaporation pressure which is eliminated at laser pulse expiration as shown in Fig. 11.

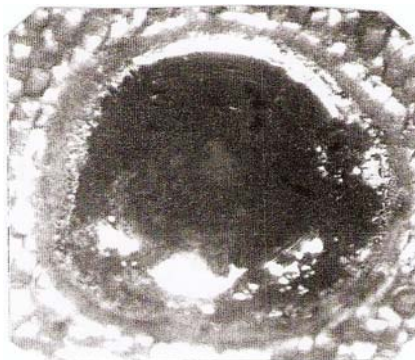


Fig. 11. PS irradiated using E.D. 1.4 J/cm^2 .



Fig. 12. PS irradiated shows the circular drops using E.D. 1.25 J/cm^2 .

The result of laser energy density of 1.25 J/cm^2 shows the emergence of a clear hole surrounded by central circles due to interference between the incident and reflected laser beam, as shown in Fig. 12.

5. Conclusions

The induced-defects generated by laser irradiation are a function of the increased laser power densities. The deficiencies are of the form of fractions and cracks caused by thermal shock. Defects emerged in the form of large crack due to the laser irradiation accumulation of heat. Defects emerged in the form of large holes due to the temperature of the irradiated region rising up to evaporation temperature in a short time. The X-ray diffraction showed the change in the phase of irradiated region from crystalline to amorphous as a function of increasing laser power density. Finally, the emergence of

induced-defects led to the increase in the surface resistivity.

Acknowledgements

The authors would like to acknowledge Universiti Sains Malaysia for a Short Term Grant No. 304/PFIZIK/637040 to support this work.

References

- [1] L. T. Canham, Appl. Phys. Lett. **57**, 1046 (1990).
- [2] Z. Ch. Feng, R. Tsu, Porous Silicon, World Scientific, Singapore, 1994.
- [3] A. G. Cullis, L. T. Canham, P. D. J. Calcott, J. Appl. Phys. **82**, 909 (1997).
- [4] G. Amato, C. Delerue, H. J. von Bardeleben, Structural and Optical Properties of Porous Silicon Nanostructures **5**(5), Yoshihiko Kanemitsu, CRC Press, 1998.
- [5] Z. Fekih, F. Z. Otmani, N. Ghellai, N. E. Chabanne-Sari, Characterisation of the porous silicon layers, 2006 Unit of research of Materials and renewable Energies (U.R.M.E.R) and University Abou - Baker Belkaid B.p: 119 TLEMCEM 13000 Algeria .
- [6] Ti. L. Rittenhouse, P. W. Bohna, T. K. Hossain, I. Adesida, J. Lindesay, A. Marcus, J. of Appl. Phys. **95**, 490 (2004).
- [7] M. Ohmukai, M. Taniguchi, Y. Tsutsumi, Mat. Sci. Eng. **B86**, 26 (2001).
- [8] V. Lehman, U. Gosele, Appl. Phys. Lett. **58**, 856 (1991).
- [9] T. H. Gfroerer, Encyclopedia of Analytical Chemistry R. A. Meyers Ed., John Wiley & Sons Ltd, Chichester, 9209 (2000).
- [10] M. Yang, D. Huang, P. Hao, F. Zhang, X. Hou, Surface Physics Laboratory, Fudan University, Shanghai 200433, China, 1993.
- [11] R. Prabakaran, R. Kesavamoorthy, Alok Singh, Bull. Mater. Sci. **28**(3), 219(2005).
- [12] K. W. Cheah, T. Chan, W. L. Lee, Appl. Phys. Lett. **63**(25), 3464 (1993) .
- [13] C. H. Chen, Y. F. Chen, Solid State Commun. **111**, 681 (1998).
- [14] I. K. Meshkovskii, O. V. Klim, S. N. Dmitriev, Tech. Phys. Lett. **23**, 11 (1997).
- [15] Sh. D. Milani , R. S. Dariani, A. Mortezaali, V. Daadmehr, K. Robbie, J. Optoelectron. Adv. Mater. **8**(3), 216 (2006).
- [16] R. T. Young, R. F. Wood, Annual Review of Materials Science **12**, 323 (1982).
- [17] V. Lo, Y. W. Wong, H. Cho, Y. Q. Chem., K. Y. Tong, Simeconductor. Sci. Technol. **H**, 1285 (1996).
- [18] John C. Ion, Laser Processing of Engineering Materials, Butterworth-Heinemann, 2005.

*Corresponding author: asmat_hadithi@yahoo.com